DOI: 10.1002/ejic.200600592

Testing Phosphanes in the Palladium-Catalysed Allylation of Secondary and Primary Amines

Claire Thoumazet,[a] Hansjörg Grützmacher,[b] Bernard Deschamps,[a] Louis Ricard,[a] and Pascal le Floch*[a]

Keywords: Allylation / Amines / Catalysis / Palladium / Phosphorus

The electronic nature of the ligand plays a crucial role in the palladium-catalysed allylation of amines with allylic alcohols. The better the ligand is as a π acceptor, the more active the catalyst. Experiments with a series with mono- and bidentate ligands featuring phosphanes and phospholes applied in the catalytic allylation of aniline clearly demonstrate this. Bolstered by DFT calculations, we have devised a new efficient catalyst for this process which carries the strong π acceptor 1,2,5-triphenylphosphole as a ligand.

Introduction

Carbon–nitrogen bond formation is a major challenge in organic synthesis for the preparation of nitrogen containing molecules of biological and physiological interest.[1] Among various metal promoted catalytic processes, the Tsuji–Trost[1a,2] coupling reaction involving the reaction of a nucleophile with a transient allyl palladium complex proves to be one of the most straightforward routes towards allylamines. Various nucleophiles and protected allylic alcohols can be employed and this reaction usually proceeds with good conversion under mild conditions.[3] However, as in other allylic alkylation processes, the presence of a good leaving group such as carboxylate, carbonate, phosphate or other related derivatives on the allylic moiety is a prerequisite in most cases in order to obtain sufficient activity. From a practical, economical and environmental point of view an interesting goal consists of directly using allylic alcohols as alkylating agents.[4] This approach has been explored by Tamaru as well as Ozawa and Yoshifuji in 2002. Tamaru et al. showed that classical palladium(0) complexes, such as $Pd(PPh_3)_4$ and $Pd(OAc)_2/PnBu_3$, could be employed as catalysts for the allylation of primary and secondary amines using a variable amount of BEt_3 (between 0.3 and 2.4 equiv.) as a cocatalyst. The group of Ozawa demonstrated that DPCB Pd(allyl) complexes (DPCB stands for diphosphanylidenecyclobutene ligands) efficiently catalyse the coupling between aniline derivatives and allylic alcohols in the presence of $MgSO_4$ as a water scavenger to afford the corresponding allylamines in good yields (Scheme 1).[4a–4d] Recently, we showed that allyl palladium complexes of mixed bidentate P-S ligands featuring a phosphabarrelene moiety and a diphosphanyl sulfide pendant arm are efficient catalysts for the bis(allylation) of primary amines under mild conditions.[5]

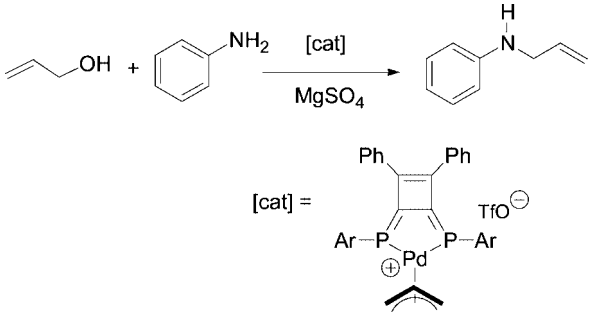

Scheme 1. Allylation of primary amines by DPCB based complexes.

Though the mechanism of this new catalytic process has not been explored in detail, the experimental results suggest that the π accepting capacity of the ligand likely plays a decisive role in the outcome of the reaction. That is, the stronger the π accepting capacity, the faster the process. In this article we report on the use of mono- and bidentate ligands in this allylation process and show through DFT calculations that the electronic nature of the phosphane indeed plays a crucial role. As will be seen, these studies led

[a] Laboratoire "Hétéroéléments et Coordination" UMR CNRS 7653, École Polytechnique,
91128 Palaiseau Cedex, France
Fax: +33-1-69-33-39-90
E-mail: lefloch@poly.polytechnique.fr
[b] Department of Chemistry and Applied Biosciences (D-CHAB), ETH Hönggerberg,
Wolfgang-Pauli Str., 8093 Zürich, Switzerland
Fax: +41-1-633-10.32
E-mail: gruetzmacher@inorg.chem.eth.ch
Supporting information for this article is available on the WWW under http://www.eurjic.org or from the author.

us to devise a new efficient catalyst featuring the easily available 1,2,5-triphenylphosphole[6] as a ligand.

Results and Discussion

Synthesis of Complexes

All experiments were carried out using cationic palladium(allyl) complexes as precursors. As neutral donor ligands, various acyclic and cyclic phosphanes and one 1,4-diazabutadiene ligand **1** (Ar = 2,6-diisopropylbenzene) were tested as models for N–N chelating ligands (see Scheme 2 for a representation of all ligands employed in this study). The classical triphenylphosphane ligand **2** was used as a reference and its activity was compared with that of chelating ligands such as dppe **3** [dppe = 1,2-bis(diphenylphosphanyl)ethane] and dppp **4** [dppp = 1,3-bis(diphenylphosphanyl)propane] to assess the importance of the chelate effect. Furthermore, a series of phosphole based ligands was investigated including the readily available 1,2,5-triphenylphosphole **5** and the phenyldibenzophosphole **6**[7] as well as the chelate ligands **7** and **8**[8] which are the phospholyl counterparts of dppe and dppp, respectively. To complete this series, we extended our study to the 1-dibenzotropylidene-*P*-dibenzophosphole **9**, a ligand which has already proved to be very efficient in the Suzuki–Miyaura cross coupling process allowing the synthesis of arylboronic esters.[9] Note that it was shown previously that this highly rigid phosphane alkene (PAL) acts as a firmly binding bis(chelate) because of its well preorganised concave shaped binding site.

All cationic palladium complexes were conventionally prepared by treating equimolar amounts of the ligand with the $[PdCl(allyl)]_2$ dimer in dichloromethane at room temperature. After stirring for 5 min, the formation of the complexes $[Pd(allyl)(L_2)]Cl$ (L_2 = two monodentate ligands or one bidentate ligand) was verified by ^{31}P NMR spectroscopy (see the experimental section for ^{31}P NMR spectroscopic data of the intermediary complexes). Subsequently, a silver salt AgX (X = OTf or NTf_2; Tf = $-SO_3CF_3$) was added to exchange the chloride thereby affording the expected cationic complexes **10a**–**17a** (X = OTf) or **10b**–**17b** (X = NTf_2) (see Scheme 3). Complexes **10a**,**b** were isolated as orange powders in excellent yields and their structures are in accord with by NMR spectroscopy and elemental analysis. Complex **10a** was also structurally characterised (X-ray crystal structure given in the available supplementary material). Complexes **11a**,**b** were characterised by NMR spectroscopy and elemental analyses and their NMR spectroscopic data were compared with those reported in the literature for the $[Pd(PPh_3)_2(allyl)][X]$ complexes.[10] The dppe and dppp complexes **12a**,**b**, and **13a**,**b** as well as the phosphole derivatives **14a**,**b** and **15a**,**b** were synthesised by following the same experimental procedure and isolated as colourless or pale-yellow powders (fully characterised by NMR spectroscopy and elemental analyses). X-ray analyses of single-crystals of complexes **11a** (not reported in this paper), **12b** and **13a** (given in the available supplementary material) and of the phosphole complexes **14a** and **15a** were performed to elucidate their structures. The structures of the latter are presented in Figure 1 and Figure 2, respectively. Information concerning the data col-

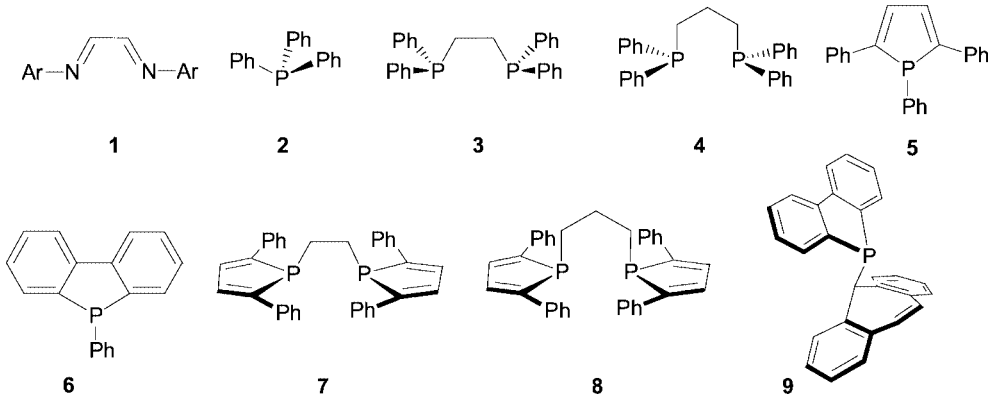

Scheme 2. Ligands used in this study.

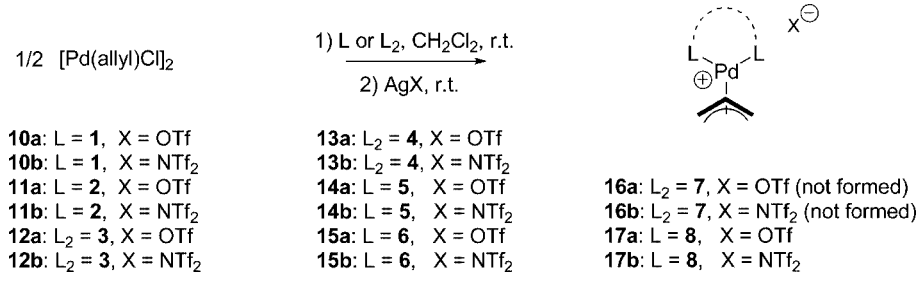

Scheme 3. Synthesis of cationic complexes **10**–**17a**,**b**.

lection and refinement are given in Table 9 for both complexes. Selected bond lengths (Å) and angles (°) are listed in Table 1 (complex **14a**) and Table 2 (complex **15a**), respectively.

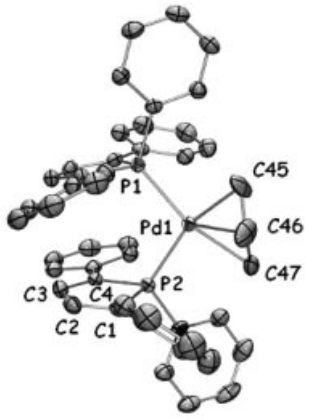

Figure 1. A view of one molecule of complex **14a**.

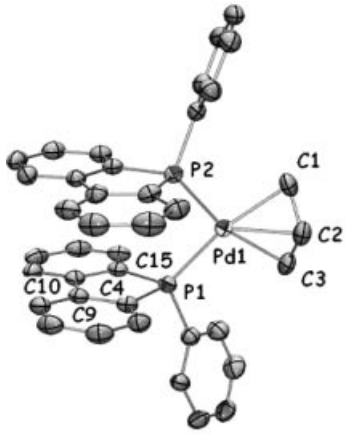

Figure 2. A view of one molecule of complex **15a**.

Table 1. Selected bond lengths [Å] and bond angles [°] for complex **14a**.

P1–Pd1	2.3066(6)	C2–C3	1.437(4)
P2–Pd1	2.3254(6)	C3–C4	1.360(3)
Pd1–C45	2.143(2)	C4–P2	1.818(2)
Pd1–C46	2.141(3)	P1–Pd1–P2	102.4(2)
Pd1–C47	2.202(3)	C45–C46–C47	123.7(3)
P2–C1	1.812(2)	C4–P2–C1	107.6(2)
C1–C2	1.348(3)	P1–Pd1–C45	130.2(1)

Table 2. Selected bond lengths [Å] and bond angles [°] for complex **15a**.

P1–Pd1	2.3096(7)	C9–C10	1.465(4)
P2–Pd1	2.2882(7)	C10–C15	1.398(4)
Pd1–C1	2.190(3)	C15–P1	1.824(3)
Pd1–C2	2.176(3)	P1–Pd1–P2	99.13(2)
Pd1–C3	2.164(3)	C1–C2–C3	121.0(3)
P2–C4	1.804(3)	C15–P1–C4	91.2(1)
C4–C9	1.405(4)	P1–Pd1–C3	67.5(1)

As displayed in Figure 1, complex **14a** adopts the expected square-planar geometry. The two phenyl rings of the phosphole ligands point in opposite directions in order to minimise the steric congestion with the second phosphole ligand. No stacking interactions between the two phosphole rings or their phenyl substituents can be observed. The P1–Pd1 and P2–Pd1 bond lengths at 2.307(1) Å and 2.325(1) Å are comparable with the corresponding Pd–P bonds in the PPh_3 complex (**11a**) [2.311(1) Å and 2.339(1) Å]. Similarly, the Pd–C_{allyl} bonds (see Table 1) fall in the same range as those of the PPh_3 complex [2.153(2), 2.174(4) and 2.236(8) Å]. Note that in the 1,4-diazabutadiene complex **10a**, the Pd–C_{allyl} bonds [2.107(3), 2.122(2) and 2.114(3) Å] are significantly shorter than in the two phosphole complexes indicating a stronger bond between the Pd atom and the allyl group.

The structure of **15a** is different and π stacking between the planar dibenzophosphole ligands can be observed (distance between the two planes: 3.66 Å). Other metric parameters are close to those recorded for the structures of complexes **11a** and **14a**. The bidentate ligands **7** and **8** have already been synthesised by Neibecker et al. following the classical procedure which consists of treating the 2,5-diphenylphospholide anion with 1,2-dibromoethane and 1,3-dibromopropane.[8] Complexes **17a**,**b** were straightforwardly formed and isolated as dark-red powders and their identities were ascertained by NMR spectroscopic studies and elemental analyses (see Scheme 3). On the contrary, the synthesis of complexes **16a**,**b** failed. Whatever the experimental conditions used, each attempt led to the formation of dark solids that could not be dissolved in common organic solvents and despite many efforts, the insoluble materials could not be characterised.

The synthesis of complexes **19a**,**b** took a slightly different reaction pathway. Specifically, the reaction of ligand **9** with $[Pd(allyl)Cl]_2$ did not yield a cationic complex with chloride as the counter-anion but the neutral species **18** which results from the breaking of the dimer, the chloride ligand remaining coordinated to the palladium centre (see Scheme 4). Complex **18** was characterised by ^{31}P NMR spectroscopy and its structure determined by an X-ray diffraction study.

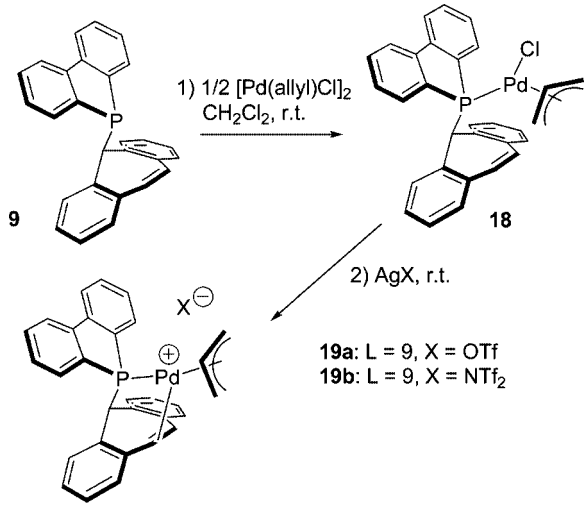

Scheme 4. Synthesis of cationic complexes **18** and **19a**,**b**.

Figure 3 shows the result and selected bond lengths and angles are listed in Table 3. The structure of complex **18** shows that the 1-dibenzotropylidene-*P*-dibenzophosphole is coordinated to the metal centre by means of the phosphorus atom only, the C=C_{trop} unit remaining uncoordinated. In order to minimise repulsive steric interactions, the tropylidene and the allyl fragment point in opposite directions with respect to the central plane through the Pd atom.

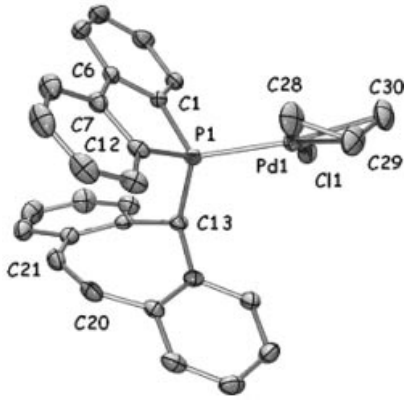

Figure 3. A view of one molecule of complex **18**.

Table 3. Selected bond lengths [Å] and bond angles [°] for complex **18**.

P1–Pd1	2.2822(6)	Pd1–C29	2.170(4)
P1–C1	1.813(2)	Pd1–C30	2.215(4)
C1–C6	1.407(3)	Pd1–Cl1	2.3767(7)
C6–C7	1.466(3)	C20–C21	1.337(4)
C7–C12	1.403(3)	C28–C29–C30	120.5(7)
C12–P1	1.811(2)	C1–P1–C12	91.6(1)
P1–C13	1.875(2)	P1–Pd1–C28	96.7(2)
Pd1–C28	2.104(5)	P1–Pd1–C30	164.0(2)

Treatment with one equivalent of AgX (X = OTf, NTf_2) yielded the expected cationic species **19a**,**b** which were isolated as very stable colourless powders (see Scheme 4). The coordination of the double bond to the metal was ascertained by NMR studies and is also seen in the solid-state structure of complex **19b** (Figure 4). Selected bonding parameters are listed in Table 4. Details concerning the crystal data collection and refinement are given in Table 9.

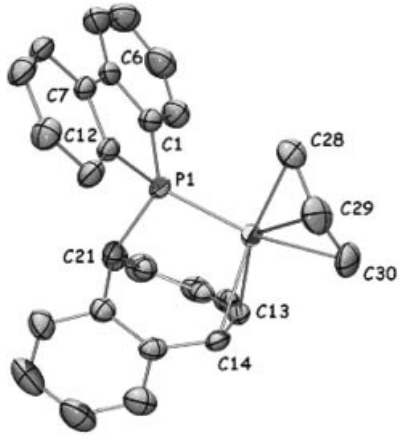

Figure 4. A view of one molecule of complex **19b**.

Table 4. Selected bond lengths [Å] and bond angles [°] for complex **19b**.

P1–Pd1	2.272(1)	Pd1–C30	2.214(4)
P1–C1	1.815(4)	Pd1–C13	2.306(3)
C1–C6	1.406(5)	Pd1–C14	2.293(3)
C6–C7	1.468(6)	C13–C14	1.380(6)
C7–C12	1.415(5)	C28–C29–C30	120.2(5)
C12–P1	1.788(4)	C1–P1–C12	92.1(2)
P1–C21	1.866(4)	C13–Pd1–C14	34.9(1)
Pd1–C28	2.135(4)	P1–Pd1–C28	99.0(1)
Pd1–C29	2.166(4)	P1–Pd1–C30	165.9(1)

The metric parameters of complex **19b** are comparable with those found in complex **15a**. The C=C_{trop} bond length of the tropylidene unit [1.380(6) Å] is slightly lengthened when compared with the uncoordinated C=C_{trop} bond in **18** indicating π back donation from the metal fragment to the ligand.

Catalytic Experiments

Having all these complexes at hand, we investigated their performance in catalytic allylic aminations. The allylation of aniline was chosen as a model reaction (Scheme 5). All experiments were carried under the same experimental conditions, that is, in THF or toluene at room temperature with $MgSO_4$ as a water scavenger using 1 mol-% of catalyst, two equiv. of aniline and one equiv. of allylic alcohol. These conditions are similar to those used by Ozawa et al. during their studies with the above mentioned DPCB complexes. The use of two equiv. of aniline disfavours the formation of the bis(allylation) derivatives.

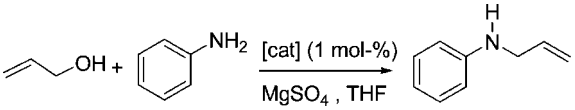

Scheme 5. Catalytic coupling of allyl alcohol with aniline using palladium allyl complexes **10a**,**b**–**19a**,**b** as catalyst precursors.

A first series of experiments showed that the use of toluene or THF as solvent had no influence and gave similar results. Therefore, all subsequent experiments were performed in THF. As shown in Table 5, only catalysts **11a**,**b**, **14a**,**b**, **15a**,**b** and **19b** gave a complete or nearly complete conversion (80 to 100%) after a reaction time of 24 h. In the experiments with **11a**,**b**–**17a**,**b**, the nature of counteranion did not have a significant influence on the catalytic performance. However, under the reaction conditions used in these experiments, a strong influence was seen with complexes **19a**,**b**, where the triflate derivative **19a** gave only a 20% conversion (vide supra).

Table 5. Conversion in the catalytic coupling of allyl alcohol with aniline using palladium allyl complexes **10a**,**b**–**19a**,**b** as catalyst precursors. (n.t. = not tested).

Catalyst	24 h	1 h	Catalyst	24 h	1 h
10a	0%	n.t.	14a	100%	72%
10b	0%	n.t.	14b	100%	100%
11a	100%	47%	15a	100%	52%
11b	80%	27%	15b	85%	34%
12a	20%	n.t.	17a	73%	18%
12b	5%	n.t.	17b	69%	13%
13a	5%	n.t.	19a	20%	n.t.
13b	2%	n.t.	19b	98%	30%

Hard σ donor ligands such as the diazadiene ligand in complexes **10a**,**b** are not suited to the Pd-catalysed allylation of aniline and no conversion was achieved. Complexes such as **12a**,**b** and **13a**,**b** with bidentate ligands also showed very low activities with conversions not exceeding 20%. The chelate complexes **17a**,**b** carrying the bis(phosphole) ligand **8** gave better results but no complete conversion was observed after 24 h.

In a second series of experiments, the most active catalysts were selected and the reaction was stopped after 1 h. As the results in Table 5 show, catalyst **14b** proved to be the most active (complete conversion) and, as previously observed with **19a**,**b**, this complex with the NTf_2 counteranion was more active than its triflate counterpart **14a** (72%). However, complete conversion with **14a** was achieved after 2 h. The second best catalyst in terms of efficiency is the dibenzophosphole based complex **15a** which afforded a conversion of 52%. In this case, the NTf_2 derivative **15b** was less active (34%). The triphenylphosphane complex **11a** (47% of conversion) ranks in third place. Among the complexes which showed substantial conversion after 1 h reaction time, complex **19b** was the least efficient catalyst (30%). Note that in all these experiments the addition of $MgSO_4$ is not necessary and the absence of this water scavenger resulted only in a small decrease in the conversion yields (about 10%).

Having identified **14b** as an efficient catalyst, some additional experiments were also conducted with a lower loading of catalyst (0.5 and 0.1 mol-%) and by varying the substitution scheme of the allyl alcohol. These results are presented in Scheme 6. Longer reaction times or heating were needed to achieve a nearly complete conversion when a low loading of the catalyst was used (7 h at room temp. with 0.5 mol-% of catalyst and 5 h at 70 °C with 0.1 mol-% of catalyst). Methylallyl alcohol and *trans*-crotyl alcohol were also used as substrates. Introduction of a methyl group at the alpha position of the alcohol resulted in a significant decrease in the catalytic activity and, after 24 h at room temp., only 40% of the substrate was converted. As previously observed by Ozawa and Yoshifuji, introduction of a methyl group at the β position (*trans*-crotyl alcohol) leads to a mixture of SN_2 and SN_2' products in a 71:12 ratio.

To complete this study, we then focused our efforts on the bis(allylation) of primary amines as well as on the monoallylation of secondary amines. This latter transformation is known, in particular, to be much more difficult to achieve.[4c–4d,5] For the bis(allylation) process, catalyst **14b** (1 mol-%) was treated with one equiv. of amine and two or three equiv. of the allylic alcohol in THF at room temperature with $MgSO_4$. With two equiv. of alcohol a nearly complete conversion was obtained after 39 h of stirring [92% of bis(allylation), 8% of monoallylation]. With three equiv. a complete conversion could be obtained after 14 h of reaction (see Scheme 7).

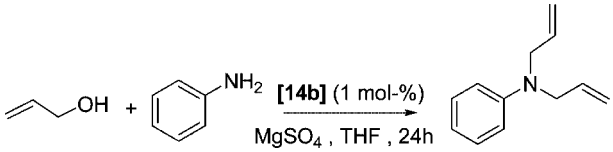

Scheme 7. Bis(allylation) of primary amines with catalyst **14b**.

Experiments to test the activity of **14b** in the allylation of secondary amines were conducted with 1 mol-% of catalyst, one equiv. of amine and two equiv. of allyl alcohol in THF (at room temperature and 50 °C) in the presence of $MgSO_4$. Three amines were tested: morpholine, dibenzylamine and *N*-methylaniline. A complete conversion was obtained after 24 h of heating at 50 °C with morpholine and *N*-methylaniline as substrates. Note that **14b** is therewith the most efficient catalyst reported to date for this transformation.[5] All the results are summarised in Table 6.

The results from the catalyses clearly demonstrate that the electronic nature of the phosphane plays a crucial role for the activity. As previously observed, strong π acceptor ligands lead to higher TON (TON = turn over numbers). Because diarylalkyl-substituted phosphanes such as dppe, dppp and ligand **8** show weaker π accepting capacities than triaryl phosphanes, the better performance of $[Pd(C_3H_5)(PPh_3)_2][X]$ **11a**,**b** can be explained. However, the

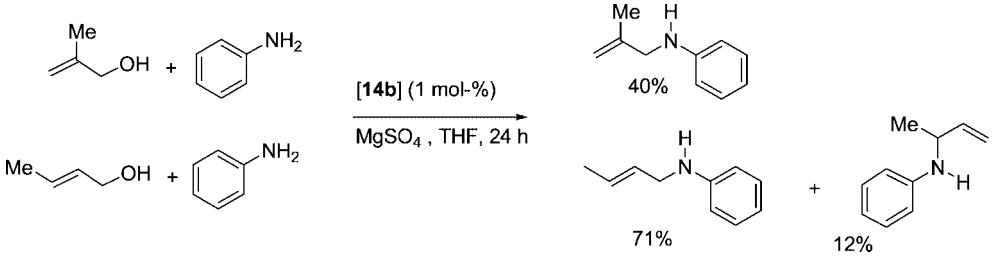

Scheme 6. Reaction of aniline with methyl alcohol and *trans*-crotyl alcohol catalysed by complex **14b**.

Table 6. Conversion in the catalytic coupling of allyl alcohol with secondary amines with **14b** as a catalyst precursor.

Secondary amines	Temperature	Conversion
N-Methylaniline	room temp.	100%
Morpholine	room temp.	28%
Morpholine	50 °C	100%
Dibenzylamine	room temp.	11%
Dibenzylamine	50 °C	44%

explanation of the especially high activity of catalyst precursor **14** with the 2,5-diphenylphosphanylphosphole **5** as ligand as compared with **15** with the dibenzophosphole derivative **6** is less straightforward and requires a better understanding of the electronic nature of the ligands. Consequently, a DFT study was carried out.

DFT Calculations

Calculations were carried out at the B3PW91/6-31G* level of theory using the Gaussian 03 set of programs. Views of the two calculated structures are shown in Figure 5 and selected bond lengths and angles are listed in Table 7. The agreement between the calculated and experimentally found bonding parameters[11] is satisfactory. Because of the nonplanarity of the phosphorus atom, phospholes are weakly aromatic.[12] The aromaticity of phospholes has been the subject of many debates and several factors determine the degree of aromaticity, such as the substitution pattern at the carbon atoms, the pyramidalisation of the coordination sphere at phosphorus and, most importantly, the nature of the substituent at phosphorus which determines the amplitude of the overlap between the π system of the C_4-butadienyl fragment and the P–R bond. This has been recently demonstrated with a series of 1-R–P substituted phospholes.[13] Both **5** and **6** carry a phenyl group as the substituent, hence the degree of deviation φ of the P–C bond from the ring plane can be used in first approximation as an indicator. Thus **5** (φ = 68°) would show a higher degree of aromaticity than **6** (φ = 72°). The significantly lower inversion barrier at the phosphorus atom for **5** (16.9 kcal mol^{-1}) than in **6** (26.2 kcal mol^{-1}) supports this conclusion (see the supporting information for a presentation and structure parameters of the transition states of the inversions calculated at the same level of theory). Two explanations can be proposed to rationalise the weaker inversion barrier in phosphole **5**. First one may propose that the higher barrier for **6** is the result of significant overlap between the σ-P–R bond and the π system of the butadienyl fragment (negative hyperconjugation) which stabilises the ground state of this less aromatic ring system. Note that the inversion barrier for triphenylphosphane **2** was found to be equivalent to that of **6**, that is 26.2 kcal mol^{-1}. A second possibility is to consider that in the transition state the phosphole **5** is more aromatic than **6** since in this fused system the π electrons are delocalised into the two neighbouring six-membered aromatic rings.[14] To confirm our findings further, the nucleus independent chemical shifts (NICS) were calculated for both phospholes and their transition states (noted **TS5** and **TS6**, respectively). There is a good relationship between the NICS and other aromaticity criteria in phospholes and the more negative the NICS the higher the aromatic character.[15] NICS calculations were performed with the optimised structures at the RHF/6-311+G** level of theory (measured at 1 Å above the plane defined by the ring, opposite to the substituent at phosphorus). Table 8 shows that phosphole **5** is more aromatic than **6**. Not surprisingly, the presence of two fused benzene rings in **6** decreases the aromatic character of the central phosphole nucleus. A similar phenomenon has already been reported by Schleyer in the case of other fused structures such as phenanthrene.[15b] In **6**, the NICS value of the peripheral benzene rings (–10.3) is higher than that calculated for benzene (–8.4) using the same method and basis set. NICS calculations were also performed on the two transitions states **TS5**

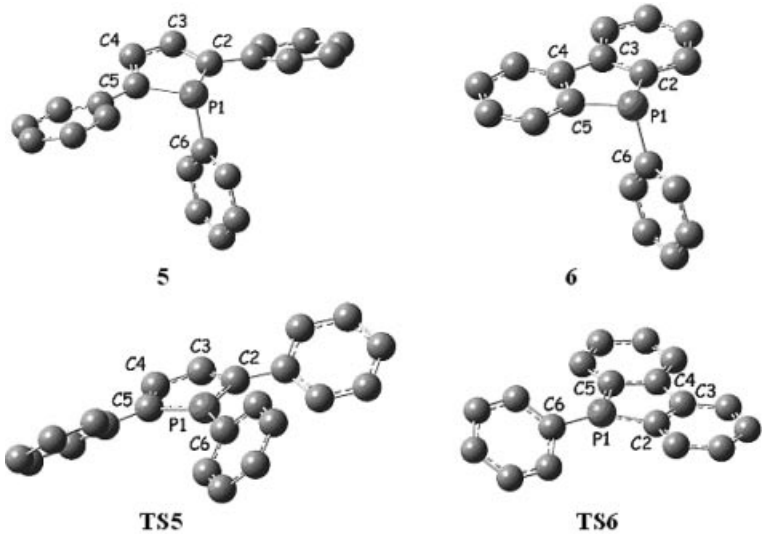

Figure 5. Views of the optimised geometries of the two ligands **5** and **6** and **TS5** and **TS6** (hydrogens have been excluded).

and **TS6**, the structures of which are also presented in Figure 5. Both transition states are, as expected, more aromatic than their respective precursors but the differences between the NICS values are insignificant (NICS for **TS5**: –9.0; NICS for **TS6** = –8.9), that is, the degree of aromaticity of the transition states is not the determining factor (see Scheme 8).

Table 7. A comparison between calculated and experimental bond lengths [Å] and angles [°] for ligands **5** and **6**.

	5 theoretical	**5**[11a] experimental	**6** theoretical	**6**[11b] experimental
P1–C2	1.822	1.822	1.832	1.812
C2–C3	1.368	1.348	1.412	1.385
C3–C4	1.441	1.440	1.469	1.465
P1–C6	1.839	1.822	1.848	1.841
C3–C2	114.8	116.1	110.0	110.2
P1–C5	1.821	1.822	1.832	1.818

Table 8. Sum of the bond angles around the P atoms, Σ° (P), deviation φ of the P–C bond out the PC_4 plane in the calculated structures of ligands **5** and **6**. NICS values and data from CDA calculations for complexes **I**, **II** and **III**. *b* and *d* values are expressed in electrons and *d*/*b* and *b*/*d*+*b* ratios are given in percent.

Ligands and complexes	**5**	**6**	**I**	**II**	**III**
Σ° (P)	302	296			
φ°	68	72			
NICS (1 Å)	– 4.3	– 2.1			
donation (d)			0.437	0.406	0.420
back-donation (b)			0.065	0.086	0.067
d/*b*			6.7	4.7	6.3
d/*d*+*b*			13	17.5	13.7
r			– 0.341	– 0.331	– 0.331
Δ			– 0.010	– 0.009	– 0.009

The binding properties of **5** and **6** towards transition metal fragments were estimated by means of a charge decomposition analysis (CDA) as developed by Frenking et al.[16] For simplicity, and in order to allow comparison with previous work, we chose, as models, the $Ni(CO)_3$ complexes **I**, **II** and **III** with triphenylphosphane **2**, triphenylphosphole **5** and dibenzophosphole **6** as ligands, respectively (Figure 6).

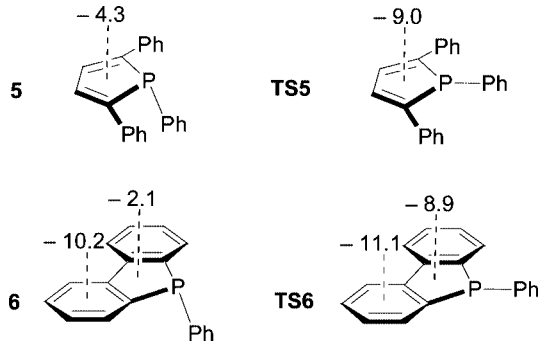

Scheme 8. NICS values calculated at the RHF/6-311+G** level of theory (measured at 1 Å above the plane defined by the ring, opposite to the substituent at phosphorus) for **5**, **6**, **TS5** and **TS6**.

Results of this CDA analysis are presented in Table 8, further details are given in the experimental section. The small residual term (Δ) in all complexes shows that the electron density has been adequately partitioned into the repulsive term, *r*, and L→M donor, *d*, as well as the M→L back-donating terms, *b*. Hence, the discussion of the data from the CDA is meaningful.

The data given in Table 8 show that the ligands PPh_3 and dibenzophosphole **6** have similar electronic properties, that is, they have similar donation/back-donation ratios, *d*/*b*, of about 6.5. The triphenylphosphole **5** is a better acceptor, its *d*/*b* ratio is significantly smaller (4.7).

Inspection of the MO's involved in the bonding in complexes **II** (HOMO-12 and HOMO-2, see Figure 7) and **III** (HOMO-11 and HOMO-2) revealed that, as expected, the most significant contribution to the bonding comes from the orbital which describes the lone pair at phosphorus, i.e. the HOMO-1 in **5** and the HOMO in **6**. On the other hand, the π back donation mainly results from the combination of a filled orbital of the $Ni(CO)_3$ fragment with the LUMO+7 of **5** and **6** (σ* orbitals).

In summary, the results from the DFT calculations fully support the idea that the π accepting capacity of the ligand governs the catalytic activity of the palladium complexes prepared from them: while $[Pd(C_3H_6)(PPh_3)_2]X$ **10a**,**b** and $[Pd(C_3H_6)(\mathbf{6})]X$ **15a**,**b** perform similarly, $[Pd(C_3H_3)(\mathbf{5})]$ **14a**,**b** stands out with its exceptional activity.

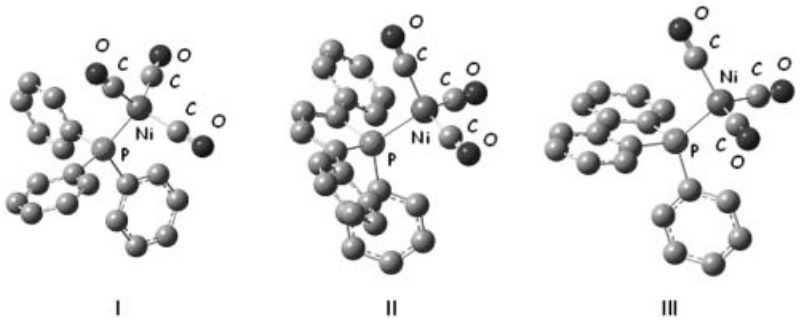

Figure 6. Views of the optimised geometries of the complexes **I**, **II** and **III** (hydrogen atoms have been excluded).

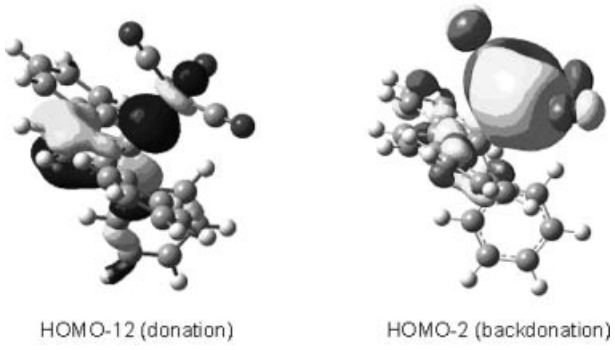

Figure 7. Views of the two MO's which describe the bonding in complex **II**.

Conclusions

The performance of a series of catalysts with different phosphane ligands and one complex with a diazabutadiene ligand was evaluated in the palladium catalysed allylation of primary and secondary amines. In this way, a new efficient catalyst carrying the 1,2,5-triphenylphosphole **5** as a ligand (complexes **14a**,**b**) was found which enables these coupling reactions under mild conditions. DFT calculations enabled a comparison of the electronic structures of the ligands which gave the most active catalysts and, in combination with calculations on simple model complexes, strongly support the proposition that the best catalysts are obtained with π accepting ligands. Further studies will now focus on a systematic investigation of other strong π acceptor ligands, especially suitably substituted phospholes and phosphanes. Though significant progress has been achieved through this study, the influence of the ligands and their related complexes on the mechanistic pathway has yet to be precisely assessed as well as details on the stereochemical course of the reaction. DFT calculations aimed at determining the whole catalytic cycle of this important transformation are currently underway and will be presented in due course.

Experimental Section

General Remarks: All reactions were routinely performed under an inert atmosphere of argon or nitrogen by using Schlenk and glovebox techniques and dry deoxygenated solvents. Dry THF and hexanes were obtained by distillation from Na/benzophenone. Dry dichloromethane was distilled from P_2O_5, dry toluene from Na and dry acetonitrile from CaH_2. NMR spectra were recorded on a Bruker Avance 300 spectrometer operating at 300 MHz for ^1H, 75.5 MHz for ^{13}C and 121.5 MHz for ^{31}P. Solvent peaks were used as internal references relative to Me_4Si for ^1H and ^{13}C chemical shifts (ppm). ^{31}P chemical shifts are relative to an 85% H_3PO_4 external reference and coupling constants are expressed in Hertz. Abbreviations used: b broad, s singlet, d doublet, t triplet, m multiplet, p pentuplet, sext sextuplet, sept septuplet, v virtual. Elemental analyses were performed by the Service d'analyse du CNRS at Gif sur Yvette, France. $[Pd(COD)Cl_2]$,[17] *P*-phenyldibenzophosphole (**6**),[7] (dibenzo[*a*,*d*]cyclohepten-5-yl)dibenzophosphole (**9**),[9] triphenylphosphole (**5**),[6] diazadiene (**1**)[18] and (2,5-diphenylphosphol-1-yl)alkanes **7** and **8**[8] were prepared according to literature procedures. All other reagents and chemicals were obtained commercially and used as received. The GC yields were determined on a Varian Star 3400 gas chromatograph equipped with a CHROMPACK column (column type: WCOT FUSED SILICA, stationary phase: CP-SIL 5 CB).

Theoretical Methods: The calculations were performed with the GAUSSIAN 03 series of programs.[19] The geometries of compounds **2** and **5** and **6** were optimised by using the B3PW91 functional.[20] The standard 6-31G* basis set was used for all atoms (H, C and P). NICS calculations were performed at the RHF/6-311+G** level of theory using geometries calculated at the RB3PW91/6-31G* level of theory. The $Ni(CO)_3$ complexes **I**, **II** and **III** were calculated with the B3PW91 functional using the 6-31+G** basis set for P atoms, the 6-31G** basis set for the carbonyl groups and the 6-31G basis set for the H and C atoms. The basis set for the metal was that associated with the pseudo potential, with a standard double-ζ LANL2DZ contraction. In each case, harmonic frequencies were calculated at the same level of theory to characterise the stationary points and to determine the zero-point energies (ZPE). Intrinsic reaction coordinate calculations (IRC) were performed to ensure that transition states were found for the inversion at the phosphorus atoms in the structures of **5** and **6**. All optimised structures reported here have only positive eigenvalues of the Hessian matrix, i.e they are minima on the potential energy surface. Inspection of ligand to metal donor-acceptor interactions were performed using the charge-decomposition analysis (CDA). In the CDA method the (canonical, natural or Kohn–Sham) molecular orbitals of the complex are expressed in terms of MO's of appropriately chosen fragments. In the cases studied, the Kohn–Sham orbitals of the calculations are formed in the CDA procedure as a linear combination of the MO's of the phosphorus ligands **2**, **5** and **6** and those of the remaining $[Ni(CO)_3]$ fragment. In all cases, the ligands and the metal fragments were computed in the geometry of the complex. The orbital contributions are divided into four parts: (i) the mixing of the occupied MO's of the ligand and the unoccupied MO's of the metal fragment. This value (noted *d*) represents the L→M donation; (ii) the mixing of the unoccupied MO's of the ligand and the occupied MO's of the metal fragment. This value (noted *b*) accounts for the M→L back donation; (iii) the mixing of the occupied MO's of the ligand and the occupied MOs of the metal fragment. This term (noted *r*), which describes the repulsive polarisation between the ligand and metal fragment, is negative because electronic charge is removed from the overlapping area of the occupied orbitals; (iv) the residual term (Δ) which results from the mixing of the unoccupied MO's of the two respective fragments. Usually this term is very close to zero for closed-shell interactions. This value constitutes an important probe for determining whether the bonding studied can be really classified as a donor-acceptor interaction following the Dewar–Chatt–Duncansson model. Important deviations from $\Delta = 0$ imply that the bond studied is more conventionally described as a normal covalent bond between two open shell fragments. A more detailed presentation of the CDA method and the interpretation of the results can be found in the literature. Compositions of molecular orbitals, overlap populations between molecular fragments, bond orders and density-of-states spectra were calculated by using the AOMix program developed by I. Gorelski (version 6.23).[21]

X-ray Structure Data: Nonius KappaCCD diffractometer, φ and ω scans, Mo-K_α radiation ($\lambda = 0.71073$ Å), graphite monochromator, $T = 150$ K, structure solution with SIR97,[22] refinement against F^2 in SHELXL97[23] with anisotropic thermal parameters for all non-hydrogen atoms, calculated hydrogen positions with riding isotropic thermal parameters (Table 9).

Table 9. Crystal data for complexes **14a**, **15a**, **18** and **19b**.

	14a	**15a**	**18**	**19b**
Empirical formula	$C_{47}H_{39}P_2Pd$, CF_3O_3S, CH_2Cl_2	$C_{39}H_{31}P_2Pd$, CF_3O_3S	$C_{30}H_{23}ClPPd$	$C_{30}H_{24}PPd$, $C_2F_6NO_4S_2$
Molecular mass [g mol^{-1}]	1006.12	817.05	556.30	802.05
Crystal size [mm]	0.20 × 0.18 × 0.18	0.23 × 0.20 × 0.03	0.20 × 0.18 × 0.18	0.22 × 0.16 × 0.16
Crystal colour and shape	yellow block	light yellow plate	yellow plate	colourless block
Crystal system	monoclinic	monoclinic	monoclinic	monoclinic
Temperature [K]	150.0(1)	150.0(1)	150.0(1)	150.0(1)
Space group	$P2_1/n$	$P2_1$	$P2_1$	$P2_1/c$
a [Å]	12.2870(10)	11.6440(10)	9.4010(10)	44.9220(10)
b [Å]	22.1630(10)	11.8720(10)	13.9750(10)	14.9800(10)
c [Å]	16.1300(10)	13.8110(10)	10.0440(10)	18.8280(10)
β [°]	93.9700(10)	110.7300(10)	115.3000(10)	97.6100(10)
V [Å^3]	4381.9(5)	1785.6(3)	1193.00(19)	12558.4(11)
Z	4	2	2	16
Density (calculated) [g cm^{-3}]	1.525	1.520	1.549	1.697
Absorbtion coefficient [mm^{-1}]	0.722	0.722	0.974	0.851
F(000)	2048	828	562	6431
θ max [°]	30.03	27.45	30.03	27.48
Reflections collected [$I \geq 2\sigma(I)$]	21134	8000	5637	45074
Independent reflections	12788 [R_{int} = 0.0208]	8000 [R_{int} = 0.0000]	5637 [R_{int} = 0.0000]	26730 [R_{int} = 0.0164]
Data/restraints/parameters	9168/16/550	7463/16/466	5344/17/309	20798/13/1558
Gof on F^2	1.039	1.024	1.055	1.042
R(F), $R_w(F^2)$ [$I \geq 2\sigma(I)$]	0.0439, 0.1281	0.0293, 0.0730	0.0252, 0.0636	0.0503, 0.1609
Largest diff peak/hole [e Å^{-3}]	1.549(0.092)/ –0.986(0.092)	0.633(0.057)/ –0.637(0.057)	0.509(0.067)/ –0.626(0.067)	2.068(0.110)/ –0.757(0.110)

CCDC-294689 to -294695 contain the crystallographic data for the structures reported in this paper and have been deposited with the Cambridge Crystallographic Data Centre. Copies of these data can be obtained free of charge from The Cambridge Crystallographic Data Centre via www.ccdc.cam.ac.uk/data_request/cif.

Synthesis of Complexes 10a,b [Pd(1)(η_3-C_3H_5)][X]: To a solution of glyoxal-bis(2,6-diisopropylphenyl)imine (100 mg, 0.26 mmol) in dichloromethane (2 mL) was added $[Pd(allyl)Cl]_2$ (48.6 mg, 0.13 mmol). After 5 min stirring, the silver salt AgX (0.26 mmol, **10a**: 68.2 mg, **10b**: 99.3 mg) was added and the pale-yellow solution became orange. Filtration of AgCl on celite followed by evaporation of the dichloromethane yielded the complexes as orange powders in very good yields (**10a**: 97%, 170 mg; **10b**: 98%, 201 mg). Single-crystals of **10a** were obtained by slow diffusion of hexanes into a solution of the complex in chloroform at room temperature. ^{1}H NMR ($CDCl_3$, 25 °C): δ = 1.32 (m, 24 H, CHCH_3), 3.03 (m, 2 H, CHCH$_3$), 3.17 (vd, AA′BB′C, Σ J = 12.8 Hz, 2 H, CH_{allyl}), 3.25 (m, 2 H, CHCH$_3$), 3.59 (vd, AA′BB′C, Σ J = 7.0 Hz, 2 H, CH_{allyl}), 5.56 (tt, J = 7.0 and 12.8 Hz Hz, 1 H, CH_{allyl}), 7.26–7.40 (m, 6 H, m-Ph), 8.61 (s, 2 H, CH=N) ppm. ^{13}C NMR ($CDCl_3$, 25 °C): δ = 23.0 (CHCH$_3$), 23.7 (CH=N), 28.9 (CHCH$_3$), 65.1 (CH_{2allyl}), 120.1 (CH_{allyl}), 124.1–128.8 (m-Ph), 138.1 (o-Ph), 146.1 ($ipso$-Ph), 170.0 (p-Ph) ppm. $C_{30}H_{41}F_3N_2O_3PdS$ (673.14): calcd. C 53.53, H 6.14; found C 53.28, H 6.12.

Synthesis of Complexes 12a,b [Pd(3)(η_3-C_3H_5)][X]: To a solution of 1,2-bis(diphenylphosphanyl)ethane (100 mg, 0.25 mmol) in dichloromethane (2 mL) was added $[Pd(allyl)Cl]_2$ (0.13 mmol, 45.9 mg). After stirring for 5 min, the formation of a bidentate complex was confirmed by ^{31}P NMR (δ = 51.2 ppm). The silver salt AgX was then added (0.25 mmol, **12a**: 64.5 mg, **12b**: 93.9 mg). Filtration of AgCl on celite followed by evaporation of the dichloromethane yielded the complexes as white powders in very good yields (**12a**: 98%, 170 mg; **12b**: 98%, 200 mg). Single-crystals of **12b** were obtained by slow diffusion of hexanes into a solution of the complex in dichloromethane at room temperature. ^{31}P NMR ($CDCl_3$, 25 °C): δ = 51.4 ppm. ^{1}H NMR ($CDCl_3$, 25 °C): δ = 2.70 (m, $A_2A'_2XX'$, Σ J = 99.5 Hz, 4 H, CH_2PPh$_2$), 3.39 (vddd, AA′BB′CXX′, ΣJ = 24.8 Hz, 2 H, CH_{allyl}), 4.86 (m, AA′BB′CXX′, Σ J = 12.4 Hz, 2 H, CH_{allyl}), 5.81 (vtt, $AB_2C_2X_2$, Σ J = 42.5 Hz, 1 H, CH_{allyl}), 7.43–7.60 (m, 20 H, Ph) ppm. ^{13}C NMR ($CDCl_3$, 25 °C): δ = 27.5 (vt, AXX′, Σ J = 46.0 Hz, CH_2PPh), 71.4 (vt, AXX′, Σ J = 33.2 Hz, CH_{2allyl}), 123.6 (vt, AXX′, Σ J = 12.2 Hz, CH_{allyl}), 129.9–132.8 (Ph) ppm. $C_{31}H_{29}F_6NO_4P_2PdS_2$ (826.1): calcd. C 45.07, H 3.54; found C 44.85, H 3.53.

Synthesis of Complexes 13a,b [Pd(4)(η_3-C_3H_5)][X]: To a solution of 1,2-bis(diphenylphosphanyl)propane (100 mg, 0.24 mmol) in dichloromethane (2 mL) was added $[Pd(allyl)Cl]_2$ (0.12 mmol, 44.5 mg). After 5 min stirring, the formation of a bidentate complex was confirmed by ^{31}P NMR (δ = 6.3 ppm). The silver salt AgX was then added (0.24 mmol, **13a**: 61.7 mg, **13b**: 89.8 mg). Filtration of AgCl on celite followed by evaporation of the dichloromethane yielded the complexes as white powders in very good yields (**13a**: 96%, 165 mg; **13b**: 95%, 190 mg). Single-crystals of **13a** were obtained by slow diffusion of hexanes into a solution of the complex in dichloromethane at room temperature. ^{31}P NMR ($CDCl_3$, 25 °C): δ = 6.8 ppm. ^{1}H NMR ($CDCl_3$, 25 °C): δ = 2.00 (m, $A_2M_4X_2$, Σ J = 147.7 Hz, 2 H, CH_2CH$_2$PPh$_2$), 2.76 (m, $A_2A'_2M_2XX'$, Σ J = 87.4 Hz, 4 H, CH$_2$CH_2PPH$_2$), 3.28 (vddd, AA′BB′CXX′, Σ J = 25.6 Hz, 2 H, CH_{allyl}), 3.95 (vddd, AA′BB′CXX′, Σ J = 13.5 Hz, 2 H, CH_{allyl}), 5.7 (vtt, $AB_2C_2X_2$, Σ J = 42.2 Hz, 1 H, CH_{allyl}), 7.31–7.48 (m, 20 H, Ph) ppm. ^{13}C NMR ($CDCl_3$, 25 °C): δ = 18.7 (s, CH$_2$CH$_2$PPh$_2$), 25.3 (vt, AXX′, Σ J = 30.7 Hz, CH$_2$CH_2PPh$_2$), 73.7 (vt, AXX′, Σ J = 32.5 Hz, CH_{2allyl}), 123.0 (vt, AXX′, Σ J = 12.4 Hz, CH_{allyl}), 128.9–132.8 (Ph) ppm. $C_{31}H_{31}F_3O_3P_2PdS$ (709.0): calcd. C 52.51, H 4.41; found C 52.35, H 4.40.

Synthesis of Complexes 14a,b [Pd(5)(η_3-C_3H_5)][X]: To a solution of $[Pd(allyl)Cl]_2$ (0.16 mmol, 58.6 mg) in dichloromethane (2 mL) was added triphenylphosphole (0.32 mmol, 100 mg). The formation of the monophosphole complex was confirmed by ^{31}P NMR (δ = 20.9 ppm). A second equiv. of triphenylphosphole (0.32 mmol, 100 mg) was added and after 5 min stirring, the formation of the

bis(phosphole) complex was confirmed by ^{31}P NMR (δ = 11.0 ppm). The chloride was then abstracted with a silver salt AgX (0.32 mmol, **14a**: 83 mg, **14b**: 120 mg). Filtration of AgCl on celite followed by evaporation of the dichloromethane yielded the complexes as yellow powders in very good yields (**14a**: 98%, 280 mg; **14b**: 95%, 325 mg). Single-crystals of **14a** were obtained by slow diffusion of hexanes into a solution of the complex in dichloromethane at room temperature. ^{31}P NMR (CD_2Cl_2, 25 °C): δ = 22.7 ppm. ^1H NMR (CD_2Cl_2, 25 °C): δ = 3.61 (vdd, AA′BB′CXX′, ΣJ = 22.5 Hz, 2 H, CH_{allyl}), 4.61 (vdd, AA′BB′CXX′, ΣJ = 9.5 Hz, 2 H, CH_{allyl}), 5.75 (vsept, $AB_2C_2X_2$, ΣJ = 41.9 Hz, 1 H, CH_{allyl}), 6.88 (m, $A_2A'_2XX'$, ΣJ = 68.9 Hz, 4 H, H_β), 7.03–7.32 (m, 30 H, H_{Ph}) ppm. ^{13}C NMR (CD_2Cl_2, 25 °C): δ = 80.1 (vt, AXX′, ΣJ = 25.8 Hz, CH_{2allyl}), 122.8 (vt, AXX′, ΣJ = 9.9 Hz, CH_{allyl}), 126.7 (vt, AXX′, ΣJ = 7.5 Hz, CH_{Ph}), 127.0 (vt, AXX′, ΣJ = 7.4 Hz, CH_{Ph}), 129.0 (s, CH_{Ph}), 129.1 (s, CH_{Ph}), 129.2 (s, CH_{Ph}), 129.6 (vt, AXX′, ΣJ = 10.9 Hz, CH_{Ph}), 131.9 (s, CH_{Ph}), 132.4 (vt, AXX′, ΣJ = 11.6 Hz, C_{Ph}), 133.1 (vt, AXX′, ΣJ = 14.4 Hz, C_{Ph}), 133.2 (vt, AXX′, ΣJ = 14.4 Hz, C_{Ph}), 135.0 (vt, AXX′, ΣJ = 13.5 Hz, CH_β), 135.4 (vt, AXX′, ΣJ = 13.4 Hz, CH_β), 142.6 (m, ΣJ = 121.7 Hz, Cα) ppm. $C_{48}H_{39}F_3O_3P_2PdS$ (921.3): calcd. C 62.58, H 4.27; found C 62.18, H 4.25.

Synthesis of Complexes 15a,b [Pd(6)(η_3-C_3H_5)][X]: To a solution of $[Pd(allyl)Cl]_2$ (0.14 mmol, 50 mg) in dichloromethane (2 mL) was added the 1-phenyl dibenzophosphole (0.27 mmol, 71 mg). The formation the monophosphole complex was confirmed by ^{31}P NMR (δ = 15.8 ppm). A second equiv. of 1-phenyl dibenzophosphole (0.27 mmol, 71 mg) was added and after 5 min stirring, the formation of the bis(phosphole) complex was confirmed by ^{31}P NMR (δ = 11.9 ppm). The chloride was then abstracted with a silver salt AgX (0.27 mmol, **15a**: 70 mg, **15b**: 102 mg). Filtration of AgCl on celite followed by evaporation of the dichloromethane yielded the complexes as pale yellow powders in very good yields (**15a**: 98%, 217 mg; **15b**: 97%, 245 mg). Single-crystals of **15a** were obtained by slow diffusion of hexanes into a solution of the complex in dichloromethane at room temperature. ^{31}P NMR (CD_2Cl_2, 25 °C): δ = 13.9 ppm. ^1H NMR (CD_2Cl_2, 25 °C): δ = 3.84 (br. s, 4 H, CH_{allyl}), 5.71 (vq, $AB_2C_2X_2$, ΣJ = 41.9 Hz, 1 H, CH_{allyl}), 7.68–7.21 (m, 26 H, Ph) ppm. ^{13}C NMR (CD_2Cl_2, 25 °C): δ = 74.23 (br. s, CH_{2allyl}), 121.0 (br. s, CH_{allyl}), 122.2 (d, J_{PH} = 5.0 Hz, CH_{Ph}), 129.1 (d, J_{PH} = 11.2 Hz, CH_{Ph}), 129.3 (d, J_{PH} = 12.3 Hz, CH_{Ph}), 131.1 (br. s, CH_{Ph}), 131.3 (s, CH_{Ph}), 131.6 (vt, AXX′, ΣJ = 11.9 Hz, CH_{Ph}), 142.7 (d, J_{PH} = 8.7 Hz, C_{Ph}) ppm. $C_{40}H_{31}F_3O_3P_2PdS$ (817.1): calcd. C 58.80, H 3.82; found C 58.57, H 3.82.

Synthesis of Complexes 17a,b [Pd(8)(η_3-C_3H_5)][X]: To a solution of bis(2,5-diphenylphosphol-1-yl)propane (100 mg, 0.20 mmol) in dichloromethane (2 mL) was added $[Pd(allyl)Cl]_2$ (0.10 mmol, 35.7 mg). After 15 min stirring, the silver salt AgX was added (0.10 mmol, **17a**: 50.2 mg, **17b**: 73 mg) and the formation of the complexes were confirmed by ^{31}P NMR (δ = 9.0 ppm). Filtration of AgCl on celite followed by evaporation of the dichloromethane yielded the complexes as dark-red powders in very good yields (**17a**: 95%, 150 mg; **17b**: 96%, 174 mg). ^{31}P NMR ($CDCl_3$, 25 °C): δ = 9.0 ppm. ^1H NMR ($CDCl_3$, 25 °C): δ = 2.24 [m, 6 H, $P(CH_2)_3P$], 3.19 (vdt, AA′BB′CXX′, ΣJ = 23.5 Hz, 2 H, CH_{allyl}), 4.17 (vd AA′BB′CXX′, ΣJ = 7.0 Hz, 2 H, CH_{allyl}), 5.58 (vsept, $AB_2C_2X_2$, ΣJ = 41.1 Hz, 1 H, CH_{allyl}), 7.15–7.45 (m, 24 H, Ph and H_β) ppm. ^{13}C NMR ($CDCl_3$, 25 °C): δ = 19.1 (vt, AXX′, ΣJ = 29.4 Hz, CH_2CH_2P), 20.3 (s, CH_2CH_2P), 75.3 (vt, AXX′, ΣJ = 25.6 Hz, CH_{2allyl}), 121.9 (vt, AXX′, ΣJ = 9.1 Hz, CH_{allyl}), 126.3 (m, CH_{Ph}), 128.0 (s, CH_{Ph}), 128.7 (vd, ΣJ = 10.1 Hz, CH_{Ph}), 132.5 (vt, AXX′, ΣJ = 14.6, C_{Ph}), 132.9 (vt, AXX′, ΣJ = 14.6, C_{Ph}), 134.9 (vt, AXX′, ΣJ = 14.6 Hz, CH_β), 135.6 (vt, AXX′, ΣJ = 14.8 Hz, CH_β), 144.9 (m, ΣJ = 86.7 Hz, Cα) ppm. $C_{41}H_{35}F_3O_3P_2PdS$ (833.2): calcd. C 59.11, H 4.23; found C 58.88, H 4.22.

Synthesis of Complexes 19a,b [Pd(9)(η_3-C_3H_5)][X]: To a solution of ligand (100 mg, 0.27 mmol) in dichloromethane (2 mL) was added $[Pd(allyl)Cl]_2$ (0.13 mmol, 48.8 mg). After stirring for 5 min, the formation of the intermediate complex **18** was confirmed by ^{31}P NMR (δ = 49.5 ppm) and single-crystals of **18** were grown by slow diffusion of hexanes into a solution in dichloromethane at room temperature. The chloride was then abstracted with a silver salt AgX (0.27 mmol, **19a**: 68.6 mg, **19b** 100 mg). Filtration of AgCl on celite followed by evaporation of the dichloromethane yielded the complexes as white powders in very good yields (**19a**: 97%, 175 mg; **19b**: 96%, 205 mg). Single-crystals of **19b** were obtained by slow diffusion of hexanes into a solution of the complex in dichloromethane at room temperature.

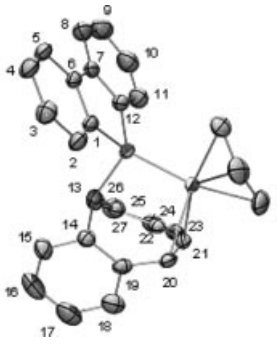

^{31}P NMR (CD_2Cl_2): δ = 55.8 ppm. ^1H NMR (CD_2Cl_2): δ = 3.25 (m, 2 H, CH_{allyl}), 4.10 (vdd, ABCDEX, ΣJ = 23.4 Hz, 1 H, CH_{allyl}), 4.62 (d, J_{PH} = 15.8 Hz, 1 H, H^{13}), 5.43 (vt, ABCDEX, ΣJ = 13.6 Hz, 1 H, CH_{allyl}), 5.77 (vsept, ABCDEX, ΣJ = 41.9 Hz, 1 H, CH_{allyl}), 6.08 (dd, $J_{H,H}$ = 7.5, $J_{P,H}$ = 7.5 Hz, 2 H, H^5–H^8), 7.01 (m, ΣJ = 10.5 Hz, 2 H, H^{15}–H^{26}), 7.15 (m, ΣJ = 21.3 Hz, 2 H, H^3–H^{10}), 7.53 (m, 6 H, H^{17}–H^{24}, H^{16}–H^{25} and H^4–H^9), 7.66 (s, 2 H, H^{20}–H^{21}), 7.72 (m, ΣJ = 8.9 Hz, 2 H, H^{18}–H^{23}), 7.95 (m, ΣJ = 9.6 Hz, 2 H, H^2–H^{11}) ppm. ^{13}C NMR (CD_2Cl_2, 25 °C): δ = 54.8 (d, $J_{P,C}$ = 14.2 Hz, C^{13}), 66.0 (s, CH_{2allyl}), 85.9 (d, J_{PC} = 24.7 Hz, CH_{2allyl}), 104.3 (s, C^{20}–C^{21}), 122.3 (d, $J_{P,C}$ = 6.1 Hz, C^2–C^{11}), 124.9 (d, $J_{P,C}$ = 5.3 Hz, C^3–C^{10}), 129.0 (d, $J_{P,C}$ = 10.5 Hz C^{15}–C^{26}), 129.5 (d, $J_{P,C}$ = 2.4 Hz, C^4–C^9), 130.8 (d, $J_{P,C}$ = 22.2 Hz, C^5–C^8), 130.9 (d, $J_{P,C}$ = 2.7 Hz, C^{16}–C^{25}), 131.8 (d, $J_{P,C}$ = 45.9 Hz, C^1–C^{12}), 131.9 (d, $J_{P,C}$ = 4.5 Hz, C^{18}–C^{23}), 132.9 (d, $J_{P,C}$ = 2.1 Hz, C^{17}–C^{24}), 133.5 (d, $J_{P,C}$ = 9.2 Hz, C^{14}–C^{27}), 135.3 (d, $J_{P,C}$ = 2.8 Hz, C^{19}–C^{22}), 142.8 (d, $J_{P,C}$ = 9.6 Hz, C^6–C^7) ppm, missing CH_{allyl}. $C_{32}H_{24}F_6NO_4PPdS_2$ (802.1): calcd. C 47.92, H 3.02; found C 47.57, H 3.01.

General Procedure for Catalytic Reactions: The catalyst (1 mol-%) was placed in a Schlenck tube with $MgSO_4$ (0.25 g) and THF (1 mL). The Schlenck tube was then filled with aniline (182 μL, 2 mmol) and allyl alcohol (68 μL, 1 mmol). The mixture was stirred at room temperature and the progress of the reaction was monitored by GC. The mixture was filtered to remove the $MgSO_4$ and the solvent evaporated in vacuo. The product was then isolated by column chromatography on alumina (hexanes).

***N*-(2-Propenyl)aniline:** See ref.[4a]

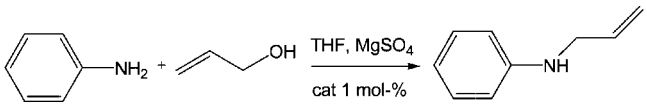

***N*,*N*-Bis(2-propenyl)aniline:** See ref.[4a]

(*E*)- and (*Z*)-*N*-(2-Butenyl)aniline and *N*-(1-Methyl-2-propenyl)aniline: See ref.[4a]

***N*-(2-Propenyl)morpholine:** See ref.[5]

***N*-(2-Propenyl)dibenzylamine:** See ref.[5]

***N*-(2-Propenyl)methylaniline:** See ref.[5]

***N*-(2-Methyl-2-propenyl)aniline:** ^{1}H NMR ($CDCl_3$): δ = 1.80 (s, 3 H, H^4), 3.69 (s, 2 H, H^1), 4.02 (br. s, 1 H, NH), 4.89 (d, J = 1.0 Hz, 1 H, H^3), 4.97 (d, J = 1.0 Hz, 1 H, H^3), 6.63 (AA′BB′C, ΣJ = 8.5 Hz, 2 H, *m*-Ph), 6.71 (tt, AB_2C_2, ΣJ = 16.8 Hz, 1 H, *p*-Ph), 7.18 (AA′BB′C, ΣJ = 15.9 Hz, 2 H, *o*-Ph) ppm. ^{13}C NMR ($CDCl_3$, 25 °C): δ = 20.6 (s, C^4), 50.1 (s, C^1), 111.1 (s, C^3), 113.0 (s, *m*-Ph), 117.5 (s, *p*-Ph), 129.3 (s, *o*-Ph), 142.8 (s, C^2), 148.2 (s, *ipso*-Ph) ppm.

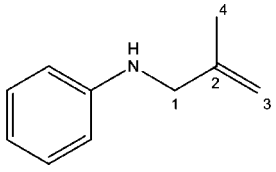

Supporting Information Available (see footnote on the first page of this article): ORTEP views and Crystallographic data for **10a**, **12b** and **13a** and optimised geometries and frequencies for compounds **5** and **6**, and for the transition states of the inversion of **5** and **6** and for the nickel complexes **I**, **II** and **III.**

Acknowledgments

The authors thank the CNRS (Centre National de la Recherche Scientifique) and the École Polytechnique for the financial support of this work, the ETH Hönggerberg (Zürich, Switzerland) and IDRIS (Orsay, Paris XI) for the allowance of computer time.

[1] a) B. M. Trost, *Chem. Pharm. Bull.* **2002**, *50*, 1–14; b) M. Johannsen, K. A. Jorgensen, *Chem. Rev.* **1998**, *98*, 1689–1708; c) B. M. Trost, D. L. Van Vranken, C. Bingel, *J. Am. Chem. Soc.* **1992**, *114*, 9327–9343; d) B. M. Trost, in: *Advances in Natural Product Chemistry* (Ed.: Atta-Ur-Rahman), Harwood Academic Publishers, Harwood, **1992**, pp. 19–34; e) S. A. Godleski, in: *Comprehensive Organic Synthesis*, vol. 4 (Eds.: B. M. Trost, I. Fleming), Pergamon Press, New York, **1991**, pp. 585–661.

[2] a) B. M. Trost, D. L. Van Vranken, *Chem. Rev.* **1996**, *96*, 395–422; b) B. M. Trost, F. D. Toste, A. B. Pinkerton, *Chem. Rev.* **2001**, *101*, 2067–2096; c) S. A. Godleski, in: *Comprehensive Organic Synthesis*, vol. 4, chapter 3.3 (Eds.: B. M. Trost, I. Fleming, M. F. Semmelhack), Pergamon Press, Oxford, **1990**; d) J. A. Davis, in: *Comprehensive Organometallic Chemistry II*, vol. 9 (Eds.: E. W. Abel, F. G. A. Stone, G. Wilkinson), Pergamon, Oxford, **1995**, p. 291; e) J. Tsuji, *Transition Metal Reagents and Catalysts*, Wiley, New York, **2000**; f) B. M. Trost, *Science* **1991**, *254*, 1471; g) B. M. Trost, *Angew. Chem. Int. Ed. Engl.* **1995**, *34*, 259–281.

[3] a) J. C. Hierso, A. Fihri, R. Amardeil, P. Meunier, H. Doucet, M. Santelli, *Tetrahedron* **2005**, *61*, 9759–9766; b) M. Feuerstein, D. Laurenti, H. Doucet, M. Santelli, *Tetrahedron Lett.* **2001**, *42*, 2313–2315; c) J. Tsuji, *Palladium Reagents and Catalysis: Innovations in Organic Synthesis* Wiley, Chichester, **1995**, p. 292; d) T. Ohmura, J. F. Hartwig, *J. Am. Chem. Soc.* **2002**, *124*, 15164–15165; e) T. Ohmura, J. F. Hartwig, *J. Am. Chem. Soc.* **2003**, *125*, 3426–3427; f) R. Kuwano, K. I. Uchida, Y. Ito, *Org. Lett.* **2003**, *5*, 2177–2179.

[4] a) F. Ozawa, H. Okamoto, S. Kawagishi, S. Yamamoto, T. Minami, M. Yoshifuji, *J. Am. Chem. Soc.* **2002**, *124*, 10968–10969; b) F. Ozawa, T. Ishiyama, S. Yamamoto, S. Kawagishi, H. Murakami, M. Yoshifuji, *Organometallics* **2004**, *23*, 1698–1707; c) H. Bricout, J.-F. Carpentier, A. Mortreux, *J. Mol. Catal. A* **1998**, *136*, 243–251; d) M. Kimura, M. Futamata, K. Shibata, Y. Tamaru, *Chem. Commun.* **2003**, 234–235; e) M. Sakaibara, A. Ogawa, *Tetrahedron Lett.* **1994**, *35*, 8013–8014; f) S. C. Yang, Y. C. Tsai, *Organometallics* **2001**, *20*, 763–770; g) Y. Tamaru, *J. Organomet. Chem.* **1999**, *576*, 215–231.

[5] O. Piechaczyk, M. Doux, L. Ricard, P. Le Floch, *Organometallics* **2005**, *24*, 1204–1213.

[6] For the synthesis see B. Lukas, R. M. G. Roberts, J. Silver, A. S. Wells, *J. Organomet. Chem.* **1983**, *256*, 103–110. For applications in catalysis see: a) C. Bergounhou, D. Neibecker, R. Réau, *J. Chem. Soc., Chem. Commun.* **1988**, 1370–1372; b) D. Neibecker, R. Réau, S. Lecolier, *J. Org. Chem.* **1989**, *54*, 5208–5210; c) D. Neibecker, R. Réau, *J. Mol. Catal.* **1989**, *50*, 153–163; d) D. Neibecker, R. Réau, *New J. Chem.* **1991**, *15*, 279–281; e) A. Polo, C. Claver, S. Castillon, A. Ruiz, J. C. Bayon, J. Real, C. Mealli, D. Masi, *Organometallics* **1992**, *11*, 3525–3533; f) L. M. Wilkes, J. H. Nelson, L. B. McCusker, K. Seff, F. Mathey, *Inorg. Chem.* **1983**, *22*, 2476–2485.

[7] S. Affandi, R. L. Green, B. T. Hsieh, M. S. Holt, J. H. Nelson, *Synth. React. Inorg. Met. Org. Chem.* **1987**, *17*, 307–318.

[8] S. Bousquet, J. J. Brunet, T. Courcet, D. Neibecker, *Phosphorus Sulfur Silicon Relat. Elem.* **1998**, *142*, 117–124.

[9] C. Thoumazet, L. Ricard, H. Grutzmacher, P. Le Floch, *Chem. Commun.* **2005**, 1592–1594.

[10] a) S. Ogoshi, M. Morita, H. Kurosawa, *J. Am. Chem. Soc.* **2003**, *125*, 9020–9021; b) S. Ogoshi, K. Tsutsumi, H. Kurosawa, *J. Organomet. Chem.* **1995**, *493*, C19–C21; c) M. W. Baize, P. W. Blosser, V. Plantevin, D. G. Schimpff, J. C. Gallucci, A. Wojcicki, *Organometallics* **1996**, *15*, 164–173.

[11] a) W. P. Ozbirn, R. A. Jacobson, J. C. Clardy, *J. Chem. Soc., Chem. Commun.* **1971**, 1062; b) E. C. Alyea, G. Ferguson, J. F. Gallagher, *Acta Crystallogr., Sect. C* **1992**, *48*, 959–961.

[12] F. Mathey, *Phosphorus-Carbon Heterocyclic Chemistry: The Rise of a New Domain*, chapter 4, Pergamon Press, Amsterdam, **2001**, p. 219.

[13] E. Mattmann, F. Mathey, A. Sevin, G. Frison, *J. Org. Chem.* **2002**, *67*, 1208–1213.

[14] W. Egan, R. Tang, G. Zon, K. Mislow, *J. Am. Chem. Soc.* **1971**, *93*, 6205–6216.

[15] a) A. Dransfeld, L. Nyulaszi, P. v. R. Schleyer, *Inorg. Chem.* **1998**, *37*, 4413–4420; b) P. v. R. Schleyer, C. Maerker, A. Dransfeld, H. J. Jiao, N. Hommes, *J. Am. Chem. Soc.* **1996**, *118*, 6317–6318; c) L. Nyulaszi, *Chem. Rev.* **2001**, *101*, 1229–1246; d) M. K. Cyranski, T. M. Krygowski, A. R. Katritzky, P. v. R. Schleyer, *J. Org. Chem.* **2002**, *67*, 1333–1338; e) P. Schleyer, *Chem. Rev.* **2001**, *101*, 1115–1117.

[16] G. Frenking, N. Frölich, *Chem. Rev.* **2000**, *100*, 717–774.

[17] D. Drew, J. R. Doyle, in: *Inorganic Syntheses*, vol. 28 (Ed.: R. J. Angelici), **1990**, pp. 348–349.

[18] M. Zettlitzer, H. tom Dieck, E. T. K. Haupt, L. Stamp, *Chem. Ber.* **1986**, *119*, 1868–1875.

[19] Gaussian 03 Revision C.02, M. J. Frisch, G. W. Trucks, H. B. Schlegel, G. E. Scuseria, M. A. Robb, J. R. Cheeseman, J. A. Montgomery Jr, T. Vreven, K. N. Kudin, J. C. Burant, J. M. Millam, S. S. Iyengar, J. Tomasi, V. Barone, B. Mennucci, M. Cossi, G. Scalmani, N. Rega, G. A. Petersson, H. Nakatsuji, M. Hada, M. Ehara, K. Toyota, R. Fukuda, J. Hasegawa, M. Ishida, T. Nakajima, Y. Honda, O. Kitao, H. Nakai, M. Klene, X. Li, J. E. Knox, H. P. Hratchian, J. B. Cross, V. Bakken, C. Adamo, J. Jaramillo, R. Gomperts, R. E. Stratmann, O. Yazyev, A. J. Austin, R. Cammi, C. Pomelli, J. W. Ochterski, P. Y. Ayala, K. Morokuma, G. A. Voth, P. Salvador, J. J. Dannenberg, V. G. Zakrzewski, S. Dapprich, A. D. Daniels, M. C. Strain, O. Farkas, D. K. Malick, A. D. Rabuck, K. Raghavachari, J. B. Foresman, J. V. Ortiz, Q. Cui, A. G. Baboul, S. Clif-

ford, J. Cioslowski, B. B. Stefanov, G. Liu, A. Liashenko, P. Piskorz, I. Komaromi, R. L. Martin, D. J. Fox, T. Keith, M. A. Al-Laham, C. Y. Peng, A. Nanayakkara, M. Challacombe, P. M. W. Gill, B. Johnson, W. Chen, M. W. Wong, C. Gonzalez, and J. A. Pople, Gaussian, Inc., Wallingford CT, **2004**.

[20] a) A. D. J. Becke, *J. Phys. Chem.* **1993**, *98*, 5648–5662; b) J. P. Perdew, Y. Wang, *Phys. Rev. B* **1992**, *45*, 13244–13249.

[21] a) S. I. Gorelsky, *AOMIX: Program for Molecular Orbital Analysis*, *http://www.sg-chem.net/*, York University: Toronto, Canada, **1997**; b) S. I. Gorelsky, *J. Organomet. Chem.* **2001**, *635*, 187–196.

[22] A. Altomare, M. C. Burla, M. Camalli, G. Cascarano, C. Giacovazzo, A. Guagliardi, A. G. G. Moliterni, G. Polidori, R. Spagna, *SIR97, An Integrated Package of Computer Programs for the Solution and Refinement of Crystal Structures using Single Crystal Data*.

[23] G. M. Sheldrick, *SHELXL-97*, University of Göttingen, Göttingen, Germany, **1997**.

Received: January 17, 2006
Published Online: August 7, 2006

